online data

Comparative functional analysis of human medium-chain dehydrogenases, short-chain dehydrogenases/reductases and aldo-keto reductases with retinoids

Oriol GALLEGO*, Olga V. BELYAEVA†, Sergio PORTÉ*, F. Xavier RUIZ*, Anton V. STETSENKO†, Elena V. SHABROVA†, Natalia V. KOSTEREVA†, Jaume FARRÉS*, Xavier PARÉS* and Natalia Y. KEDISHVILI†[1]

*Department of Biochemistry and Molecular Biology, Universitat Autònoma de Barcelona, E-08193 Bellaterra, Barcelona, Spain, and †Department of Biochemistry and Molecular Genetics, Schools of Medicine and Dentistry, University of Alabama at Birmingham, Birmingham, AL 35294, U.S.A.

Retinoic acid biosynthesis in vertebrates occurs in two consecutive steps: the oxidation of retinol to retinaldehyde followed by the oxidation of retinaldehyde to retinoic acid. Enzymes of the MDR (medium-chain dehydrogenase/reductase), SDR (short-chain dehydrogenase/reductase) and AKR (aldo-keto reductase) superfamilies have been reported to catalyse the conversion between retinol and retinaldehyde. Estimation of the relative contribution of enzymes of each type was difficult since kinetics were performed with different methodologies, but SDRs would supposedly play a major role because of their low K_m values, and because they were found to be active with retinol bound to CRBPI (cellular retinol binding protein type I). In the present study we employed detergent-free assays and HPLC-based methodology to characterize side-by-side the retinoid-converting activities of human MDR [ADH (alcohol dehydrogenase) 1B2 and ADH4), SDR (RoDH (retinol dehydrogenase)-4 and RDH11] and AKR (AKR1B1 and AKR1B10) enzymes. Our results demonstrate that none of the enzymes, including the SDR members, are active with CRBPI-bound retinoids, which questions the previously suggested role of CRBPI as a retinol supplier in the retinoic acid synthesis pathway. The members of all three superfamilies exhibit similar and low K_m values for retinoids (0.12–1.1 μM), whilst they strongly differ in their k_{cat} values, which range from 0.35 min^{-1} for AKR1B1 to 302 min^{-1} for ADH4. ADHs appear to be more effective retinol dehydrogenases than SDRs because of their higher k_{cat} values, whereas RDH11 and AKR1B10 are efficient retinaldehyde reductases. Cell culture studies support a role for RoDH-4 as a retinol dehydrogenase and for AKR1B1 as a retinaldehyde reductase *in vivo*.

Key words: alcohol dehydrogenase, aldo-keto reductase, retinaldehyde, retinoic acid, retinol, short-chain dehydrogenase.

INTRODUCTION

Retinoids participate in multiple cellular functions, mainly through the activation of nuclear receptors by retinoic acid binding [1]. Depending on cellular needs, retinol obtained from the circulation or produced locally from β-carotene [2,3] is either converted into the storage form, retinyl ester, by LRAT (lecithin–retinol acyltransferase) or directed toward retinoic acid biosynthesis. This biosynthesis occurs in two steps: retinol is oxidized to retinaldehyde, and then retinaldehyde is oxidized to retinoic acid [4]. The oxidation of retinol to retinaldehyde is a reversible reaction and the rate-limiting step of retinoic acid biosynthesis [4].

CRBPs (cellular retinol binding proteins) are a group of cytosolic proteins that bind retinol and retinaldehyde with high affinity [5]. Four different types of human CRBPs have been described [5–7], but only CRBPI has been shown to have a widespread distribution. Its physiological function is not yet fully understood. It has been proposed that holoCRBPI (CRBPI-bound retinol) serves as the primary substrate for LRAT and for retinol dehydrogenases responsible for retinoic acid biosynthesis *in vivo* [4].

Members of three oxidoreductase superfamilies have been implicated in human retinol metabolism. Historically, cytosolic ADH (alcohol dehydrogenase) enzymes of the MDR (medium-chain dehydrogenase/reductase) family were the first enzymes found to be active toward retinoids [8]. Among the human MDRs, ADH4 was shown to be the most catalytically efficient retinol dehydrogenase, followed by ADH2 and ADH1 [9]. Since most ADHs prefer NAD^+, the major oxidative cofactor in the cells [10], these enzymes were proposed to function in the oxidative direction and to catalyse the conversion of retinol to retinaldehyde for retinoic acid biosynthesis. However, despite the high catalytic efficiency of ADHs, their role in retinoid metabolism has been questioned because of their high K_m values for retinoids [9] and their inability to recognize CRBPI-bound retinol as a substrate [11].

SDRs (short-chain dehydrogenases/reductases) emerged as a novel type of all-*trans*-retinol dehydrogenases when it was reported that two of its members, rat microsomal RoDH (retinol dehydrogenase)-1 and RoDH-2, were capable of oxidizing free retinol as well as retinol bound to CRBPI [4]. Three RoDH-related NAD^+-dependent SDR dehydrogenases active toward all-*trans*-retinol have been characterized in humans [12]. The reported K_m values of these SDRs for retinoids were approx. 100-fold lower than those of ADHs. The k_{cat} values for most microsomal RoDH-like SDRs have not been determined because of the difficulties with their purification. However, successful purification of a catalytically active human RoDH-4 was recently achieved by reconstitution of the purified enzyme into proteoliposomes [13]. In addition to the NAD^+-dependent SDRs, several $NADP^+$-dependent microsomal SDRs with activities toward retinoids were

Abbreviations used: ADH, alcohol dehydrogenase; AKR, aldo-keto reductase; ASMC, aortic smooth muscle cell; CBD, chitin binding domain; CRBP, cellular retinol binding protein; EST, expressed sequence tag; FBS, foetal bovine serum; GST, glutathione S-transferase; HEK, human embryonic kidney cells; holoCRBPI, retinol bound to CRBP type I; LRAT, lecithin–retinol acyltransferase; MDR, medium-chain dehydrogenase/reductase; RoDH or RDH, retinol dehydrogenase; SDR, short-chain dehydrogenase/reductase.

[1] To whom correspondence should be addressed (email nkedishvili@uab.edu).

identified. Human microsomal RDH11 (also known as prostate SDR1 and retinaldehyde reductase 1) showed a widespread expression pattern [14] and was proposed to catalyse the reduction of all-*trans*-retinaldehyde to all-*trans*-retinol in extraocular tissues.

Most recently, the $NADP^+$-dependent AKRs (aldo-keto reductases) were defined as a new group of cytosolic enzymes that could contribute to the oxidoreductive conversions of retinoids. Members of the AKR1 family, such as chicken AKR1B12 [15], human aldose reductase (AKR1B1) [16] and human small intestine aldose reductase (AKR1B10) [16], were shown to preferentially reduce retinaldehyde to retinol. The activities of AKRs toward CRBPI-bound retinoids have not yet been examined. Overexpression of AKR1B1 has been linked to different pathologies such as diabetes and atherosclerosis [17,18]. The levels of AKR1B10 have been shown to be increased in some types of human cancer [19–22].

Numerous studies were performed to clarify the relative contribution of each enzyme group to retinol metabolism. However, never before have the properties of the enzymes from the three superfamilies been compared simultaneously using the same methodology. Activities of the soluble ADH and AKR enzymes were assayed based on spectrophotometric product detection using Tween 80 to improve the solubility and stability of retinoids. Recently, Tween 80 was found to act as a competitive inhibitor of human ADH4 and ADH1 [23], suggesting that the K_m values for retinoids might have been overestimated.

In the present study, retinoid conversions by SDR enzymes were analysed by HPLC using retinoids solubilized by binding to BSA to avoid inhibiting SDR activities by detergents (N.Y. Kedishvili and W. H. Gough, unpublished work). In addition to differences in basic analytical methodology, the reaction conditions such as temperature or buffer composition were frequently varied from one group of enzymes to another. The comparison of the kinetic properties between each enzyme type was, therefore, not possible. In the present study, the activities of human enzymes from each superfamily have been characterized using the same methodology in order to compare their catalytic efficiency for the oxidation of retinol and reduction of retinaldehyde and to determine which enzymes can utilize CRBPI-bound retinoids. This is of special interest for the identification of the key steps in the regulation of the powerful retinoic acid signalling pathway.

EXPERIMENTAL

Expression and purification of AKR1B1 and AKR1B10

Escherichia coli BL21 strain was transformed with the plasmid pET16b that encoded AKR1B1 or AKR1B10 fused to the N-terminal His_{10} tag. AKRs were expressed and purified as described previously [16] using a nickel-charged chelating Sepharose® Fast Flow resin (Amersham Biosciences).

Expression and purification of ADH1B2 and ADH4

E. coli BL21 cells were transformed with the plasmid pGEX-4T-2 containing the cDNA for either ADH1B2 or ADH4, as described previously [23]. The ADH–GST fusion proteins were purified using the affinity resin glutathione–Sepharose 4B (Amersham Biosciences).

Expression and purification of microsomal SDRs

Sf9 insect cells (Invitrogen) infected with recombinant baculovirus that contained each cDNA were grown for three days at 27 °C. Cells were homogenized using a French pressure cell press and microsomes were isolated by differential centrifugation. Purification and reconstitution of human RoDH-4 into proteoliposomes has been described previously [13]. Human RDH11-His_6 was extracted from microsomal membranes using DHPC (1,2-diheptanoyl-*sn*-glycero-3-phosphocholine; Avanti Polar Lipids) and purified using an Ni–NTA (Ni^{2+}-nitrilotriacetate) metal affinity column (Qiagen) as described previously [14].

The EST (expressed sequence tag) clone C152778 encoding RDH5 was obtained from Research Genetics. The full-length cDNA was amplified using primers 5′-GCT GGA TCC ATG TGG CTG CCT CTT CTG CT-3′ (forward primer; BamHI site underlined) and 5′-AGG GAA TTC TCA GTA GAC TGC TTG GGC AG-3′ (reverse primer; EcoRI site underlined) and cloned into the pVL1393 vector (PharMingen). Preparation of the recombinant baculovirus, expression of the protein in Sf9 cells and isolation of the microsomal fraction were carried out as described previously for RoDH-4 [24].

Expression of LRAT in Sf9 cells

The EST clone with the GenBank accession number BI461423, which contained the full-length cDNA for human LRAT [25] (insert size approx. 2 kb) between the BamHI and SalI/XhoI restriction sites of pBluescriptR vector, was obtained from the A.T.C.C. (American Type Culture Collection; catalogue number MGC-33103). The coding region was amplified using primers that contained recognition sites for restriction endonucleases BglII and XbaI respectively: forward, 5′-C TAC AGA TCT ATG AAG AAC CCC ATG CTG GAG-3′ (BglII site underlined); reverse, 5′-G GGT TCT AGA TTA GCC AGC CAT CCA TAG GAA G-3′ (XbaI site underlined). Amplification was carried out for 40 cycles with denaturing at 94 °C for 1 min, annealing at 47 °C for 1 min, and extension at 72 °C for 1.5 min. The PCR product of 0.7 kb was purified by agarose gel electrophoresis and subcloned into the pUC18 vector by blunt-end ligation. The cDNA for LRAT was excised from the pUC18 vector using BglII and XbaI restriction endonucleases and cloned into the respective sites of the baculovirus transfer vector pVL1392 (PharMingen). The cDNA sequence was confirmed by sequencing. Recombinant baculovirus was prepared as described previously for RoDH-4 [24]. Expression and isolation of microsomes containing LRAT were performed essentially as described for microsomal SDRs.

Preparation of apoCRBPI and holoCRBPI

CRBP type I was expressed in *E. coli* either as an N-terminal fusion to glutathione S-transferase (GST–CRBPI) or as a C-terminal fusion to a bifunctional tag, consisting of the CBD (chitin binding domain) and the intein (CBD–intein). The GST–CRBPI construct in the pGEX-2T vector (Pharmacia) was expressed in TG-1 *E. coli* cells and the fusion protein was purified to homogeneity using affinity chromatography on a glutathione–agarose column as described previously [11]. The CRBPI–CBD–intein fusion construct in the pKYB1 vector (New England Biolabs) was expressed in BL21(DE3) cells and purified using the IMPACT™-CN protein purification system (New England Biolabs) as described previously [26]. CRBPI was released from the intein tag after the induction of the cleavage reaction with 50 mM DTT (dithiothreitol).

To prepare holoCRBPI, an aliquot (30 mg) of purified apoCRBPI was saturated with a 2-fold molar excess of all-*trans*-retinol at room temperature (23 °C) for 1 h. Unbound retinol was removed by gel-filtration on a G50 Sephadex column [13]. The A_{350}/A_{280} ratio of the holoCRBPI preparation was 1.76. HoloCRBPI was stored in small aliquots (5 mg) at − 80 °C.

Protein analysis

Protein purity was analysed using SDS/PAGE followed by staining with Coomassie Brilliant Blue (Sigma). The protein concentration of AKR and ADH preparations was determined using the Bradford assay [27]. The protein concentration of microsomes was determined using the Lowry method [28].

Enzyme kinetics

For ADHs and AKRs, standard activity assays were performed before each experiment. Ethanol was used as a substrate for ADH1B2 and ADH4, and D,L-glyceraldehyde for AKR1B1 and AKR1B10, as described previously [16,23]. The retinaldehyde reductase activity of AKRs in the presence of Tween 80 was determined by following the absorbance at 400 nm, using a Varian Cary 400 spectrophotometer, in 0.1 M sodium phosphate buffer (pH 7.5) at 25 °C, with 0.2 mM NADPH (Sigma) in 0.2 cm path length cuvettes. One unit of activity is defined as the amount of enzyme required to transform 1 μmol of substrate/min at 25 °C.

Assays of retinoid activities in the presence of BSA were performed in 90 mM potassium phosphate buffer (pH 7.4), 40 mM KCl, at 37 °C (reaction buffer), in silicone-treated glass tubes as described previously [24]. Protein used was 2 μg for AKR1B1, 20–50 ng for AKR1B10, 0.1 μg for ADH1B2, 20 ng for ADH4, 0.5–1 μg for microsomal RoDH-4 and 10–50 ng of purified RDH11, in a 0.5–2 ml reaction volume. Substrate concentrations employed were from $10 \times K_m$ to $0.1 \times K_m$. Stock solutions of retinoid substrates (Sigma) for AKRs and SDRs were prepared in ethanol. For LRAT, DMSO (Sigma) was used as a solvent [29]. To avoid competitive inhibition effects, acetone was used for ADHs. None of the solvents exceeded 1 % (v/v) in the reaction mixture and, at the concentration employed, enzyme activity was not affected. Working stock solutions of retinoids were prepared by a 10 min sonication in the reaction buffer in the presence of equimolar delipidated BSA. The actual amount of solubilized retinoid was determined based on the corresponding molar absorption coefficients at the appropriate wavelength. The following molar absorption coefficients in aqueous solutions were used: $\varepsilon_{328} = 39\,500\ M^{-1} \cdot cm^{-1}$ for all-*trans*-retinol, $\varepsilon_{400} = 29\,500\ M^{-1} \cdot cm^{-1}$ for all-*trans*-retinaldehyde, $\varepsilon_{367} = 26\,700\ M^{-1} \cdot cm^{-1}$ for 9-*cis*-retinaldehyde. The reactions were started by the addition of the cofactor and carried out for 5–30 min at 37 °C. A saturating concentration of cofactor was used for each enzyme: 0.5 mM $NADP^+$ or NADPH for AKR1B1 and AKR1B10; 2.4 mM NAD^+ or 1 mM NADH for ADH1B2; 2.4 mM NAD^+ or 1.33 mM NADH for ADH4; and 1.2 mM NAD^+ or 1 mM NADH for RoDH-4, RDH5 and RDH11.

Activities with holoCRBPI were measured as described above but in the absence of BSA. Substrate concentrations were 5 μM for SDRs, RoDH-4 and RDH5; 10 μM for purified RDH11; and 2 μM for ADH4 and AKR1B10. Protein used was 60 μg for microsomal RoDH-4 and RDH5, 2.5 μg for purified RDH11 and 0.5 μg for ADH4 and AKR1B10. All reactions were performed in 0.5 ml and incubated for 15 min, except for ADH4 with free all-*trans*-retinol, which was incubated for 10 min.

The esterification assay for human LRAT was performed in the presence of 200 μM DPPC (α-dipalmitoyl phosphatidylcholine; Sigma) [29]. The reactions were terminated by the addition of an equal volume of ice-cold methanol. Retinoids were extracted twice with two volumes of hexane, evaporated under a stream of N_2 and dissolved in 200 μl of hexane. All retinoid manipulations were performed under dim red light.

Kinetic constants were calculated using the Grafit program (version 5.0; Erithacus Software), and the results were expressed as the mean $\pm$ S.E.M of at least three independent determinations.

HPLC analysis

After extraction, retinoids were separated by chromatography on a Spherisorb S3W column (4.6 mm $\times$ 100 mm; Waters) in hexane/methyl-t-butyl ether (96:4, v/v) mobile phase, at a flow rate of 2 ml/min using Waters Alliance 2695 HPLC. Elution was monitored at 350 nm with a Waters 2996 photodiode array, except for the esterification assay, where 325 nm was used. Commercially available standards were used to identify the peaks of all-*trans*, 9-*cis*, and 13-*cis* isomers of retinol and retinaldehyde. 9-*cis*-Retinol was synthesized by enzymatic reduction of 9-*cis*-retinaldehyde catalysed by RDH11 and purified by chromatography as described above. For retinyl esters, all-*trans*-retinyl palmitate was used as a standard.

Pull-down experiments

Binding of CRBPI to RDH11 was analysed using either glutathione–Sepharose beads to pull down GST-tagged CRBPI complexed with RDH11-His_6 or using anti-His_6 antibodies to pull-down His_6-tagged RDH11 complexed with untagged apoCRBPI. For GST pull-down experiments, purified RDH11-His_6 (3 μg) was incubated with the CRBPI–GST fusion protein in PBS for 1–16 h at room temperature (23 °C) or at 4 °C. The molar ratio of GST–CRBPI to RDH11-His_6 in the mixture varied from 2:1 to 15:1. CRBPI–GST pull-down was performed by incubating the binding mixture with glutathione–Sepharose 4B beads for 30 min on an ice-bath. After rapid centrifugation at 5000 ***g*** for 1 min, supernatants were collected and Sepharose beads were washed five times with PBS. Proteins bound to the beads were eluted with 10 mM glutathione in PBS. Proteins in the supernatant and in the eluate were analysed by SDS/PAGE with subsequent silver staining of the gel.

For immunoprecipitation using monoclonal antibodies against the histidine tag (Clontech), His_6-tagged RDH11 was mixed with apoCRBPI and was allowed to bind overnight at 4 °C. Following the addition of antibodies, the mixture was incubated for 24 h at 4 °C and the RDH11-His_6–antibody complex was precipitated by binding to Protein A–agarose (Pierce Biotechnology) for 1 h at 4 °C. Proteins bound to the beads were separated from those remaining in the supernatant by centrifugation and beads were washed five times with PBS. Proteins in the supernatant and on the beads were analysed by SDS/PAGE as described above.

Cell cultures

Human ASMCs (aortic smooth muscle cells) from normal adult thoracic aortas were obtained from control heart transplant donors. Samples were provided by the Hospital Vall d'Hebron, Barcelona, Spain, according to the rules and procedures of its ethics committee and with the permission of the next-of-kin. Human ASMCs were isolated and cultured following the explant method [30]. Briefly, tunica media were isolated mechanically from human aorta and cut into small pieces. The tissue explants were cultured at 37 °C in a humidified atmosphere containing 5 % CO_2, in DMEM (Dulbecco's modified Eagle's medium; Gibco) supplemented with FBS (10 % foetal bovine serum, Gibco), 1000 units/ml penicillin and 1000 μg/ml streptomycin (Gibco). After 3 weeks, explants were removed and cells cultured to confluency. Cells at the fourth or fifth passage were subcultured at a 1:2 ratio in six-well plates. The addition of 10 % FBS and 4.5 g/l glucose was used to stimulate cell proliferation and AKR1B1 overexpression. Immunocytochemical staining with specific antibodies against smooth-muscle α-actin (Sigma) was employed as a phenotypic marker. AKR1B1 was detected with polyclonal antiserum specific against the AKR1B1 C-terminal sequence SCTSHKDYPFHEEF.

Table 1 Kinetic constants of purified AKR, MDR and SDR enzymes with retinoids

Activities were determined in 90 mM potassium dihydrogen phosphate, 40 mM potassium chloride (pH 7.4) at 37 °C. To calculate k_{cat} values, the following molecular masses were used: 80 kDa for ADHs, 38.5 kDa for AKRs and 35 kDa for SDRs. ND, not determined; NA, no activity was detected or it was less than 0.5 nmol · min^{-1} · mg^{-1}.

Substrate and parameter	Enzyme . . . AKR1B1	AKR1B10	ADH4	ADH1B2	RDH11*	RoDH-4
All-*trans*-Retinol						
K_m (μM)	NA	0.4 ± 0.1	0.3 ± 0.03	0.3 ± 0.1	0.6 ± 0.1	1.1 ± 0.1
k_{cat} (min^{-1})	NA	7.2 ± 0.3	190 ± 6	21 ± 1	11 ± 1	1.20 ± 0.02
k_{cat}/K_m (mM^{-1} · min^{-1})	NA	18000 ± 4500	640000 ± 67000	70000 ± 23000	18000 ± 3200	1100 ± 20
All-*trans*-Retinaldehyde						
K_m (μM)	1.1 ± 0.1	0.6 ± 0.1	0.8 ± 0.1	0.40 ± 0.04	0.12 ± 0.01	ND
k_{cat} (min^{-1})	0.35 ± 0.01	27 ± 1	300 ± 10	5.0 ± 0.1	18.0 ± 0.5	ND
k_{cat}/K_m (mM^{-1} · min^{-1})	320 ± 30	45000 ± 7600	378000 ± 49000	13000 ± 1300	150000 ± 13000	ND

* Data taken from [14].

The absence of AKR1B10 was shown by employing polyclonal antiserum specific against the AKR1B10 C-terminal sequence QSSHLEDYPFDAEY. Both antisera were kindly provided by Emeritus Professor T. Geoffrey Flynn (Department of Biochemistry, Queen's University, Kingston, Ont., Canada). Goat anti-rabbit IgG (H + L) peroxidase-conjugated antibody was obtained from Bio-Rad.

For measurements of RoDH-4 activity in the cells, the cDNA for RoDH-4 was stably transfected into HEK (human embryonic kidney cells)-293 (A.T.C.C.) that normally lack this enzyme. The cDNA for RoDH-4 was cloned into a eukaryotic expression vector pIRESneo (Clontech) as follows. pIRESneo was cleaved with BstXI and blunt-ended with T4 DNA polymerase, then digested with BamHI. RoDH-4 cDNA previously cloned into BglII and XbaI restriction sites of the pVL1392 vector [24] was cleaved on the 3′ end with XbaI endonuclease. The cleaved end was blunt-ended with T4 DNA polymerase, and the cDNA was excised from the pVL1392 vector by cleaving its 5′ end with BglII endonuclease. RoDH-4 cDNA with one sticky end (BglII site) and one blunt end was ligated into the BamHI (compatible with BglII) and blunt sites of pIRESneo. The final expression construct was verified by sequencing. The pIRES vector containing RoDH-4 cDNA and empty pIRESneo vector were transfected into HEK-293 cells using Lipofectamine™ and Plus™ Reagent in Opti-MEM (minimum essential medium) following the manufacturer's protocol (Invitrogen). Forty-eight hours after transfection cells received fresh MEM supplemented with 10 % horse serum and antibiotic G418 (0.4 mg/ml). At 2 weeks after plating, independent G418-resistant cell foci were isolated with cloning rings, detached with trypsin–EDTA and transferred to 96-well cluster dishes. The cloned cell lines were expanded in MEM containing G418 (0.4 mg/ml).

Retinoid assays in cell culture

ASMC were incubated for 30 min with 10 μM retinoid in the absence or presence of tolrestat. Control cells were incubated with the same proportion of ethanol that was used for retinoid and tolrestat incubations, never exceeding 0.1 % of the medium volume. RoDH-4/HEK-293 cells were incubated with 20 μM retinol for 24 h. After incubation, cells were rinsed twice in ice-cold PBS and harvested by scraping into 200 μl 0.002 % (v/v) SDS. Cell suspensions were stored frozen at − 80 °C. The thawed suspensions were sonicated in an ice-bath to complete cell lysis. Retinoids were extracted and analysed as described above. All manipulations involving retinoids were performed in a dark room under red light to prevent photoisomerization. Cellular retinoid conversion was expressed as a percentage of retinaldehyde that had been reduced to retinol, or retinol that had been oxidized to retinaldehyde.

RESULTS

Kinetic comparison of AKR, MDR and SDR activities with free retinoids

MDR and AKR enzymes and RDH11 were purified to homogeneity, as judged by denaturing gel electrophoresis, and exhibited specific activities comparable with those previously reported [14,16,20,23,31]. Purification and reconstitution of RoDH-4 into proteoliposomes was performed as described previously [13]. This preparation of RoDH-4 contained a minor contaminating protein band [13]. Therefore, the exact concentration of RoDH-4 was determined based on the calibration curve constructed from several concentrations of BSA loaded on to the same SDS/PAGE gel.

In view of the recently reported Tween 80 inhibition of ADHs [23], we first studied the effect of this detergent on the retinaldehyde reductase activity of AKRs. Similarly to ADHs, AKR1B1 and AKR1B10 were found to be strongly inhibited by Tween 80 with the apparent competitive K_i values of 0.001 % and 0.0025 % respectively (see Supplementary Figure 1 at http://www.BiochemJ.org/bj/399/bj3990101add.htm). Therefore, the kinetic constants of human AKR1B1 and AKR1B10 were re-evaluated using the detergent-free conditions previously established for microsomal SDRs [14,24,26]. Specifically, retinoid substrates were solubilized by sonication with equimolar BSA and the reaction products were analysed by HPLC. Although BSA binds retinoids and therefore decreases free retinoid concentration, we estimated that the kinetic constants shown in Table 1 would differ from the values predicted in the absence of BSA by less than 20 %, based on the reported K_d value of 2 μM for retinol binding to BSA [32].

Both AKRs were significantly more active in the reductive direction. Only AKR1B10 exhibited measurable activity with retinol with a very low K_m (0.4 μM; Table 1). The K_m values for all-*trans*-retinaldehyde were similar (0.6–1.1 μM), but the k_{cat} value of AKR1B10 was 80-fold higher than that of AKR1B1. With the k_{cat}/K_m value of 45000 mM^{-1} · min^{-1}, AKR1B10 was a catalytically efficient retinaldehyde reductase (Table 1).

In contrast, members of the human MDR family, ADH4 and ADH1B2, showed higher catalytic efficiency in the oxidative direction (Table 1). In agreement with previous studies [9], ADH4 was a more catalytically efficient enzyme than ADH1B2. Importantly, both enzymes were found to have approx. 100-fold lower K_m values (0.3–0.8 μM) for all-*trans*-retinol and

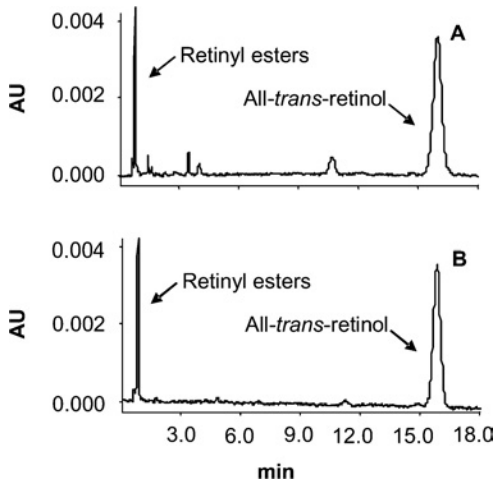

Figure 1 HPLC chromatogram showing LRAT activity

An esterification assay for microsomal LRAT was performed with 2 μM all-*trans*-retinol (**A**) or 2 μM holoCRBPI (**B**) as a substrate and 6.2 μg of microsomes containing LRAT. AU, arbitrary units.

all-*trans*-retinaldehyde than the previously reported values for Tween-solubilized retinoids [23].

Two microsomal SDR enzymes, the $NADP^+$-dependent human RDH11 and the NAD^+-dependent human RoDH-4, were also analysed. RDH11 was similar to AKR enzymes, because it preferred $NADP^+$ as a cofactor and was more efficient in the reductive direction. The catalytic efficiency of microsomal RDH11 for the reduction of all-*trans*-retinaldehyde was at least 300-fold higher than that of AKR1B1 but only 3-fold higher than that of AKR1B10 and 2-fold lower than that of ADH4 (Table 1).

In contrast, RoDH-4 was more similar to the ADH enzymes because it preferred NAD^+ as a cofactor. The apparent K_m value of RoDH-4 for all-*trans*-retinol, determined using 1 μg/ml of RoDH-4 in proteoliposomes, was 1.1 μM (Table 1), slightly higher than the K_m values of ADH enzymes.

Activity toward CRBPI-bound retinol and retinaldehyde

Since CRBPI-bound retinol had been proposed to serve as the primary substrate for retinol dehydrogenases, we tested which of the retinoid-active enzymes from AKR, MDR and SDR superfamilies could oxidize holoCRBPI. As a positive control, we employed human LRAT, which was reported to recognize holoCRBPI as a substrate [33,34]. Microsomes containing LRAT esterified 2 μM free retinol or 2 μM holoCRBPI with similar efficiency (Figure 1).

In a marked contrast to the efficient esterification of holoCRBPI, the oxidation of holoCRBPI by all three types of human oxidoreductases was much less efficient than the oxidation of unbound retinol. For example, ADH4 (0.5 μg) produced 2.3 nmol of all-*trans*-retinaldehyde from 2.5 nmol of free retinol in 10 min (Figure 2A), but only 0.17 nmol of all-*trans*-retinaldehyde from

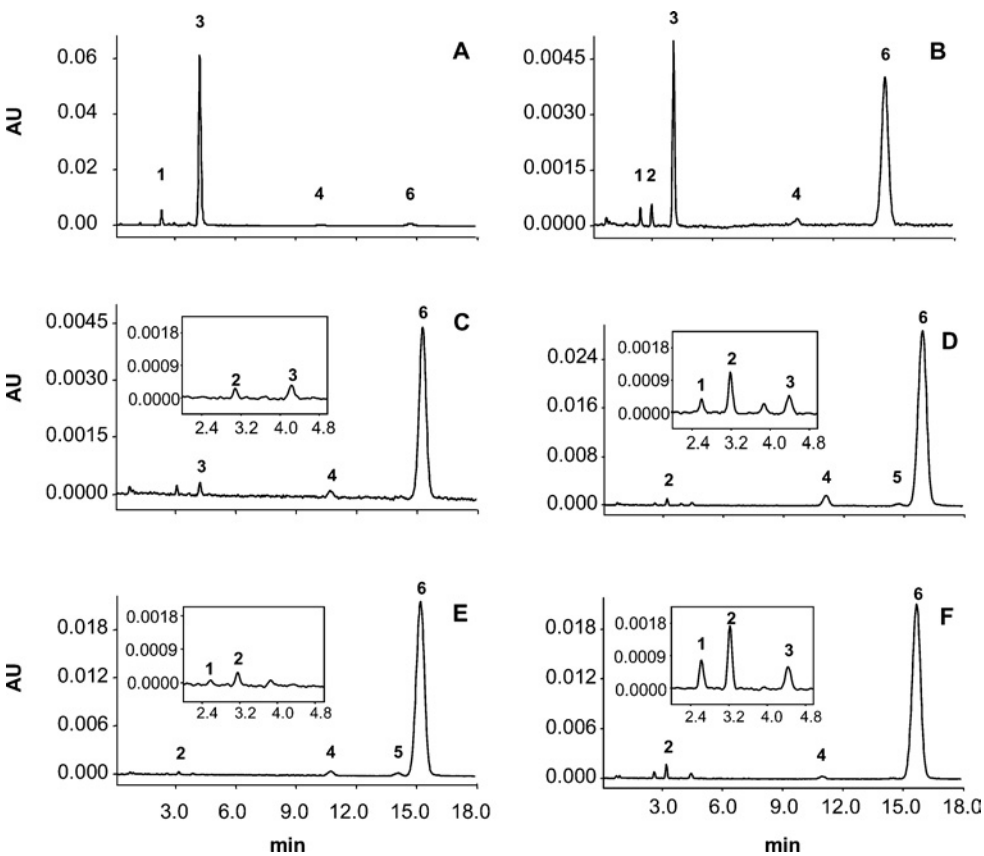

Figure 2 HPLC chromatograms showing MDR and SDR activities with all-*trans*-retinol and holoCRBPI

Activities were measured with all-*trans*-retinol, in the free form (**A**) and bound as holoCRBPI (**B**–**F**), using different enzymes: (**A**) and (**B**), ADH4; (**C**), AKR1B10; (**D**), RDH11; (**E**), RoDH-4; and (**F**), RDH5. Different isomer peaks could be identified: 1, 13-*cis*-retinaldehyde; 2, 9-*cis*-retinaldehyde; 3, -all-*trans*-retinaldehyde; 4, 13-*cis*-retinol; 5, 9-*cis*-retinol; 6, -all-*trans*-retinol. AU, arbitrary units.

Table 2 Inhibition of all-*trans*-retinaldehyde reduction by apoCRBPI

The experimental rates were determined with 0.5 μM retinaldehyde and different concentrations of apoCRBPI, in 90 mM potassium dihydrogen phosphate, 40 mM potassium chloride (pH 7.4) at 37 °C, using 0.3 μg, 80 μg, 0.5 μg and 0.19 μg of ADH4, AKR1B1, AKR1B10 and RDH11 respectively. For activity measurements in the presence of apoCRBPI, the assay mixture without cofactor was incubated for 15 min at room temperature, to ensure retinaldehyde–CRBPI binding, and the reaction was started by the addition of cofactor.

		Theoretical rate (nmol · min^{-1} · mg^{-1})†				Experimental rate (nmol · min^{-1} · mg^{-1})			
ApoCRBPI (μM)	Free retinaldehyde* (μM)	AKR1B1	AKR1B10	ADH4	RDH11	AKR1B1	AKR1B10	ADH4	RDH11
0	0.5	3	330	1400	410	4	300	900	310
0.5	0.14	1	140	530	270	0.7	90	150	240
1	0.040	0.3	50	180	130	0.2	30	16	130
2.5	0.010	0.1	15	55	50	0.06	11	10	60
10	0.006	0.05	70	25	20	0.03	5	5	20

* Theoretical amount of free all-*trans*-retinaldehyde was calculated based on the K_d value of 50 nM [5].

† Theoretical rate was calculated from the Michaelis–Menten equation using the kinetic constants determined in [14] for RDH11 and in the present study for all other enzymes.

1 nmol of holoCRBP in 15 min (Figure 2B). Under the same conditions, AKR1B10 produced only 16 pmol of all-*trans*-retinaldehyde from 1 nmol of holoCRBP (Figure 2C), whereas it produced 494 pmol of all-*trans*-retinaldehyde from 1 nmol of free retinol (results not shown). RDH11 (0.1 μg) produced 0.19 nmol of retinaldehyde from 2.5 nmol of retinol in 15 min (results not shown), but a 25-fold higher amount of RDH11 (2.5 μg) produced only 0.01 nmol of all-*trans*-retinaldehyde from 5 nmol of holoCRBP in 15 min (Figure 2D). The exact amount of retinaldehyde produced from holoCRBPI varied greatly depending on the enzyme.

These results suggested that either the enzymes utilized CRBPI-bound retinol at a much lower rate than free retinol, or that they did not use bound retinol but the amount of dissociated free retinol present in the holoCRBPI preparation was sufficient to support the observed rates. At 2 μM holoCRBPI, the concentration of unbound retinol was calculated to be 14 nM, based on the estimated K_d value of 0.1 nM for holoCRBPI [35,36]. At this concentration, the rate of retinol oxidation by ADH4 was calculated as 107 nmol · min^{-1} · mg^{-1} using the equation:

$$v = V_{max} \times [S]/(K_m + [S])$$

The rate observed in the experiment (22.7 nmol · min^{-1} · mg^{-1}) did not exceed the predicted rate, suggesting that retinaldehyde production from holoCRBPI could be fully supported by the unbound all-*trans*-retinol in the reaction mixture.

Consistent with our earlier report [13], human microsomal RoDH-4 produced retinaldehyde from holoCRBPI (Figure 2E). However, with the improved HPLC separation system employed in the present study, the predominant product of holoCRBPI oxidation was identified as 9-*cis*-retinaldehyde (Figure 2E, inset, peak 2), but not all-*trans*-retinaldehyde. This result confirmed our previous observation that holoCRBPI contains an amount of 9-*cis*-retinol that binds poorly to CRBPI [26] and that can be oxidized by *cis*-retinol-active dehydrogenases such as human microsomal RDH5 (Figure 2F) [37]. Thus, CRBPI did not affect the oxidation of *cis*-retinol but restricted the availability of all-*trans*-retinol for all human enzymes included in this study.

The effect of CRBPI on the reduction of all-*trans*-retinaldehyde by ADH4, AKR1B1, AKR1B10 and RDH11 was also tested. All-*trans*-retinaldehyde binds to CRBPI with lower affinity (K_d approx. 50 nM) than all-*trans*-retinol, and the complex of retinaldehyde with CRBPI partially dissociates during gel-filtration [26]. Therefore, for activity determinations, CRBPI was mixed with retinaldehyde directly in the assay mixture as described previously [26]. To shift the equilibrium toward bound retinaldehyde, the experiments were carried out in the presence of up to 20-fold molar excess of apoCRBPI over retinaldehyde. As shown in Table 2, the experimental rates of retinaldehyde reduction in the presence of CRBPI obtained with four different enzymes were very close to those predicted based on the calculated concentration of free retinaldehyde in the reactions. Thus, members of the three superfamilies of enzymes appeared to recognize the unbound forms of retinoids both in the oxidative and reductive directions.

To examine the possibility that CRBPI might physically interact with the oxidoreductases, we carried out pull-down assays. Purified RDH11-His$_6$ was incubated with GST-tagged or untagged CRBPI for several hours. CRBPI was then pulled down using glutathione–Sepharose beads. Alternatively, RDH11-His$_6$ was pulled down by immunoprecipitation using a monoclonal antibody against the His$_6$ tag. No binding of CRBPI to RDH11-His$_6$ was observed under any of the conditions tested. Similar results were obtained for ADH and AKR enzymes (results not shown). Consistent with the lack of protein–protein interaction between the oxidoreductases and CRBPI, 10 μM apoCRBPI had no effect on the ethanol dehydrogenase activity of ADH4, the glyceraldehyde reductase activity of AKR1B1 and AKR1B10, or the steroid dehydrogenase activity of RoDH-4 (results not shown).

Retinoid metabolism in cell cultures

With the aim to study the retinol oxidoreductase activity of AKR1B1 in a cellular environment, we prepared primary cultures of human ASMCs, known to overexpress AKR1B1 when they are stimulated to dedifferentiate and proliferate [18]. The enzyme overexpression and the absence of AKR1B10 were confirmed by Western blot analysis (results not shown). Human ASMCs were incubated with all-*trans*-retinaldehyde and the cellular retinoid content was analysed. No production of retinyl esters or retinoic acid was observed after 30 min of incubation. Human ASMC showed significant capacity for the reduction of retinaldehyde (35 % conversion of the retinaldehyde incorporated) (Figure 3A). This capacity decreased by 40 % when the cells were incubated with tolrestat, a highly specific AKR1B1 inhibitor. No retinaldehyde was formed when the cells were incubated with retinol. This observation supports the role of ARK1B1 as a retinaldehyde reductase in retinoid metabolism *in vivo*.

To study the contribution of RoDH type SDR enzymes to the metabolism of retinol in the cells, we prepared HEK-293 cells stably transfected with RoDH-4 expression vector. RoDH-4-transfected cells produced approx. 3-fold more retinoic acid than

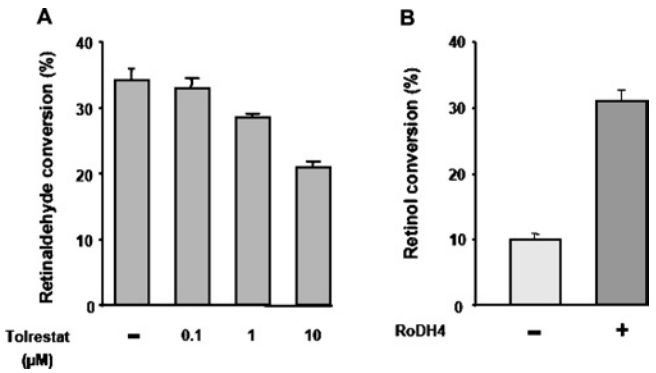

Figure 3 Retinoid metabolism in primary cultures of (A) human ASMC and (B) HEK-293 cells stably transfected with RoDH-4

mock-transfected cells (Figure 3B). This result indicated that RoDH-4 was capable of contributing to the oxidation of retinol to retinaldehyde for retinoic acid biosynthesis in the cellular context, supporting the role of RoDH-4 as a retinol dehydrogenase *in vivo*.

DISCUSSION

The present study represents the first side-by-side analysis of the catalytic properties of human retinoid oxidoreductases from three different enzyme superfamilies: MDR, SDR and AKR, with the aim to estimate their relative contribution to retinol metabolism. Although each type of retinoid oxidoreductase had been characterized before, the assay conditions and the methods used for their analysis were quite different. Kinetic analysis under detergent-free conditions now shows that different types of cytosolic and microsomal oxidoreductases all have very similar K_m values for retinol and retinaldehyde, generally, at 1 μM or below. In contrast, different enzymes have dramatically different k_{cat} values.

An important issue that has been addressed by several investigators previously is whether the retinoid-active oxidoreductases utilize retinol or retinaldehyde bound to CRBPI, allegedly the physiological form of the retinoid [4]. In the present study we have clearly demonstrated that none of the three types of human oxidoreductases oxidizes CRBPI-bound retinol or reduces CRBPI-bound retinaldehyde. In contrast, LRAT utilizes holoCRBPI almost as efficiently as free retinol. Human RoDH-4 was previously found to oxidize holoCRBPI [13,38]. However, re-examination of RoDH-4 activity in the present study revealed that the main product of holoCRBPI oxidation by RoDH-4 is 9-*cis*-retinaldehyde, but not all-*trans*-retinaldehyde. As we have reported previously, when it is exposed to light, all-*trans*-retinol isomerizes yielding 9-*cis*-retinol in the presence of CRBPI, but not in the presence of BSA [26]. With the present methodology we conclusively establish that RoDH-4 is unable to oxidize holoCRBPI.

The low K_m values suggest that ADH and SDR enzymes can effectively bind physiological levels of free retinol. As the free retinol is removed from the medium and oxidized, holoCRBPI dissociates to provide additional free retinol for retinoic acid synthesis. This outcome is consistent with the results of studies in CRBPI knockout mice which demonstrated that CRBPI is required mainly for the maintenance of the normal amount of retinol and its efficient conversion to retinyl esters for storage, but not for retinoic acid synthesis [39,40], and with the observation that several tissues with active retinoic acid synthesis do not express CRBPI [39]. In rat liver, the major storage site of retinoids, the concentration of CRBPI exceeds that of retinol (7 μM and 5 μM respectively) [41], but in limb buds of chick and mouse embryos retinol levels are much higher than the levels of CRBPI, further suggesting that unbound retinol is required as a source of retinol for retinoic acid synthesis [42].

Regarding the reducing enzymes, both cytosolic and microsomal retinaldehyde reductases can easily function in the presence of CRBPI (Table 2) because of the relatively high K_d for retinaldehyde. A physiological implication of this observation is that the presence of CRBPI appears to favour the reduction of retinaldehyde to retinol and its subsequent esterification, but it restricts the oxidation of retinol.

An unsolved issue is the relative contribution of cytosolic ADH versus microsomal RoDH enzymes to retinol oxidation. The results of knockout studies are consistent with the involvement of ADHs in retinol oxidation. ADH1, essentially a liver enzyme, is the major oxidoreductase for retinol elimination in situations of retinol excess, whilst ADH4 clearly contributes to retinoic acid biosynthesis in specific tissues [43]. ADH4 is localized in several adult epithelia that may require retinoic acid for differentiation and it is also expressed in mouse embryos in sites of retinoic acid synthesis [44]. The participation of SDRs in retinoid metabolism is supported by genetic and *in vivo* studies [45,46] and by our present cell culture results for RoDH-4. RoDH-4 is expressed in adult human liver and fetal lung. In addition, immunohistochemical analysis suggests that RoDH-4 is present in prostate epithelial cells and neurons (N. Y. Kedishvili and A. Clark, unpublished work), consistent with the ability of these cells to produce retinoic acid. RDH11 protein is expressed at relatively high levels in a wide variety of human tissues [14], all of which have active retinoid metabolism.

Comparison of the *in vitro* kinetic properties of ADHs and SDRs, obtained now under identical conditions, demonstrates similar overall kinetics, but higher k_{cat} values for ADHs and, therefore, predicts a potentially larger contribution of these enzymes. However, studies in cellular systems suggest that SDRs are more efficient than ADH4 [47]. A more relevant role for SDRs than that estimated by enzyme kinetics may be provided by their microsomal localization. An effective retinoid transfer from CRBPI to membranes exists [48], which may facilitate the utilization of retinoids by SDRs as compared to cytosolic ADHs.

We have recently recognized that several AKR members are active retinaldehyde reductases [16], thus extending the potential contribution to retinoid metabolism of another enzyme superfamily, the AKRs, in addition to MDRs and SDRs. In the present study, we provide further evidence in support of the physiological role of AKRs in the reduction of retinaldehyde. We show that AKR1B1 and AKR1B10 exhibit much lower K_m values than those previously published [16]. In addition, we demonstrate that AKR1B1 efficiently contributes to the reduction of retinaldehyde in a primary culture of human ASMCs. Therefore, despite its low k_{cat} value, the enzyme may contribute to *in vivo* retinoid metabolism, which is a relevant observation given the involvement of AKR1B1 in atherosclerosis and in the secondary pathology of diabetes.

Regarding AKR1B10, the excellent kinetic properties of the enzyme with retinaldehyde reported here, reinforces the notion that AKR1B10 could be involved in carcinogenesis by changing the flow of retinoic acid biosynthesis [49]. Tissue localization of AKR1B1 and AKR1B10 indicates that, in general, their mRNAs are expressed in a wide range of tissues although at relatively low levels [50]. This suggests a minor contribution of these enzymes to retinoid metabolism in normal tissues. This contribution would significantly increase in the above mentioned pathological conditions where the enzymes are overexpressed.

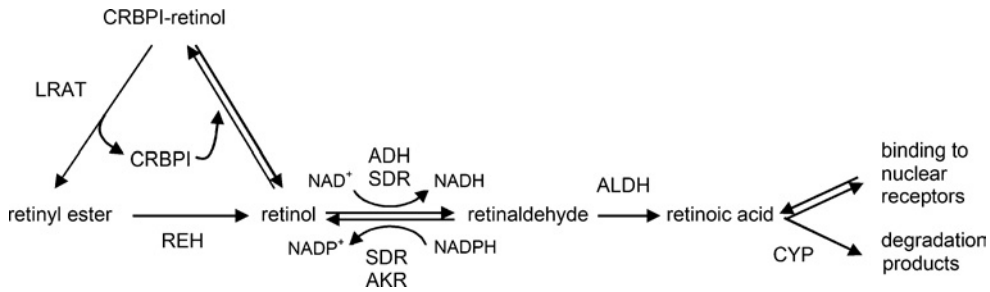

Scheme 1 Cellular retinoid metabolism

Levels of CRBPI, LRAT and oxidoreductases influence the retinoid flow either towards the storage pathway or towards retinoic acid synthesis. REH, retinyl ester hydrolase; ALDH, aldehyde dehydrogenase; CYP, cytochrome P450.

The relative amounts of LRAT, of the oxidizing enzymes (ADHs and NAD^+-dependent SDRs), the reducing enzymes (AKRs and $NADP^+$-dependent SDRs) and of CRBPI, would constitute the key factors in the control of the direction and flow of the retinoid metabolism (Scheme 1). In CRBPI knockout mice the retinoid homoeostasis is altered but the development and adult functions are normal [39]. Thus, in the absence of CRBPI, the control at the level of retinoid metabolizing enzymes may be sufficient to provide the correct amount of retinoic acid for normal functions. The multiplicity of enzyme forms from different superfamilies involved in the retinol/retinaldehyde interconversion suggests that this is an essential step that requires precise fine tuning in the pathway of retinoic acid biosynthesis.

Supported by the National Institute on Alcohol Abuse and Alcoholism, grant AA12153, and by grants from the Spanish Dirección General de Investigación (BMC2003-09606, BFU2005-02621) and the Generalitat de Catalunya (2005 SGR 00112). We thank Professor Mauro Santos (Departament de Genetica i de Microbiologia, Facultat de Ciencies Universitat Autonoma de Barcelona, Bellaterra. Barcelona, Spain) for his advice in statistical analysis and Emeritus Professor T. Geoffrey Flynn (Department of Biochemistry, Queen's University, Kingston, Ontario, Canada) for support in AKR research.

REFERENCES

1 Mangelsdorf, D., Umesono, K. and Evans, R. M. (1994) The retinoid receptors. In The Retinoids: Biology, Chemistry and Medicine (Sporn, M. B., Roberts, A. B. and Goodman, D. S., eds.), pp. 319–350, Raven Press, New York
2 Vogel, S., Gamble, M. V. and Blaner, W. S. (1999) Biosynthesis, absorption, metabolism and transport of retinoids. In Retinoids: The Biochemical and Molecular Basis of Vitamin A and Retinoid Action, vol. 139 (Nau, H. and Blaner, W. S., eds.), pp. 31–96, Springer-Verlag, Berlin
3 von Lintig, J. and Wyss, A. (2001) Molecular analysis of vitamin A formation: cloning and characterization of β-carotene 15,15′-dioxygenases. Arch. Biochem. Biophys. **385**, 47–52
4 Napoli, J. L. (1999) Interactions of retinoid binding proteins and enzymes in retinoid metabolism. Biochim. Biophys. Acta **1440**, 139–162
5 Noy, N. (2000) Retinoid-binding proteins: mediators of retinoid action. Biochem. J. **348**, 481–495
6 Folli, C., Calderone, V., Ottonello, S., Bolchi, A., Zanotti, G., Stoppini, M. and Berni, R. (2001) Identification, retinoid binding and X-ray analysis of a human retinol-binding protein. Proc. Natl. Acad. Sci. U.S.A. **98**, 3710–3715
7 Folli, C., Calderone, V., Ramazzina, I., Zanotti, G. and Berni, R. (2002) Ligand binding and structural analysis of a human putative cellular retinol-binding protein. J. Biol. Chem. **277**, 41970–41977
8 Zachman, R. D. and Olson, J. A. (1961) A comparison of retinene reductase and alcohol dehydrogenase of rat liver. J. Biol. Chem. **236**, 2309–2313
9 Yang, Z. N., Davis, G. J., Hurley, T. D., Stone, C. L., Li, T. K. and Bosron, W. F. (1994) Catalytic efficiency of human alcohol dehydrogenases for retinol oxidation and retinal reduction. Alcohol Clin. Exp. Res. **18**, 587–591
10 Veech, R. L., Eggleston, L. V. and Krebs, H. A. (1969) The redox state of free nicotinamide–adenine dinucleotide phosphate in the cytoplasm of rat liver. Biochem. J. **115**, 609–619
11 Kedishvili, N. Y., Gough, W. H., Davis, W. I., Parsons, S., Li, T. K. and Bosron, W. F. (1998) Effect of cellular retinol-binding protein on retinol oxidation by human class IV retinol/alcohol dehydrogenase and inhibition by ethanol. Biochem. Biophys. Res. Commun. **249**, 191–196
12 Kedishvili, N. Y. (2002) Multifunctional nature of human retinol dehydrogenases. Curr. Org. Chem. **6**, 1247–1257
13 Lapshina, E. A., Belyaeva, O. V., Chumakova, O. V. and Kedishvili, N. Y. (2003) Differential recognition of the free versus bound retinol by human microsomal retinol/sterol dehydrogenases: characterization of the holo-CRBP dehydrogenase activity of RoDH-4. Biochemistry **42**, 776–784
14 Belyaeva, O. V., Stetsenko, A. V., Nelson, P. and Kedishvili, N. Y. (2003) Properties of short-chain dehydrogenase/reductase RalR1: characterization of purified enzyme, its orientation in the microsomal membrane and distribution in human tissues and cell lines. Biochemistry **42**, 14838–14845
15 Crosas, B., Cederlund, E., Torres, D., Jörnvall, H., Farrés, J. and Parés, X. (2001) A vertebrate aldo-keto reductase active with retinoids and ethanol. J. Biol. Chem. **276**, 19132–19140
16 Crosas, B., Hyndman, D. J., Gallego, O., Martras, S., Parés, X., Flynn, T. G. and Farrés, J. (2003) Human aldose reductase and human small intestine aldose reductase are efficient retinal reductases: consequences for retinoid metabolism. Biochem. J. **373**, 973–979
17 Petrash, J. M., Tarle, I., Wilson, D. K. and Quiocho, F. A. (1994) Aldose reductase catalysis and crystallography. Insights from recent advances in enzyme structure and function. Diabetes **43**, 955–959
18 Ruef, J., Liu, S. Q., Bode, C., Tocchi, M., Srivastava, S., Runge, M. S. and Bhatnagar, A. (2000) Involvement of aldose reductase in vascular smooth muscle cell growth and lesion formation after arterial injury. Arterioscler. Thromb. Vasc. Biol. **20**, 1745–1752
19 Fukumoto, S., Yamauchi, N., Moriguchi, H., Hippo, Y., Watanabe, A., Shibahara, J., Taniguchi, H., Ishikawa, S., Ito, H., Yamamoto, S. et al. (2005) Overexpression of the aldo-keto reductase family protein AKR1B10 is highly correlated with smokers' non-small cell lung carcinomas. Clin. Cancer Res. **11**, 1776–1785
20 Cao, D., Fan, S. T. and Chung, S. S. (1998) Identification and characterization of a novel human aldose reductase-like gene. J. Biol. Chem. **273**, 11429–11435
21 Scuric, Z., Stain, S. C., Anderson, W. F. and Hwang, J. J. (1998) New member of aldose reductase family proteins overexpressed in human hepatocellular carcinoma. Hepatology **27**, 943–950
22 Zeindl-Eberhart, E., Haraida, S., Liebmann, S., Jungblut, P. R., Lamer, S., Mayer, D., Jager, G., Chung, S. and Rabes, H. M. (2004) Detection and identification of tumor-associated protein variants in human hepatocellular carcinomas. Hepatology **39**, 540–549
23 Martras, S., Álvarez, R., Gallego, O., Dominguez, M., de Lera, A. R., Farrés, J. and Parés, X. (2004) Kinetics of human alcohol dehydrogenase with ring-oxidized retinoids: effect of Tween 80. Arch. Biochem. Biophys. **430**, 210–217
24 Gough, W. H., VanOoteghem, S., Sint, T. and Kedishvili, N. Y. (1998) cDNA cloning and characterization of a new human microsomal NAD^+-dependent dehydrogenase that oxidizes all-*trans*-retinol and 3α-hydroxysteroids. J. Biol. Chem. **273**, 19778–19785
25 Ruiz, A., Winston, A., Lim, Y. H., Gilbert, B. A., Rando, R. R. and Bok, D. (1999) Molecular and biochemical characterization of lecithin retinol acyltransferase. J. Biol. Chem. **274**, 3834–3841
26 Belyaeva, O. V., Korkina, O. V., Stetsenko, A. V., Kim, T., Nelson, P. S. and Kedishvili, N. Y. (2005) Biochemical properties of purified human retinol dehydrogenase 12 (RDH12): catalytic efficiency toward retinoids and C9 aldehydes and effects of cellular retinol-binding protein type I (CRBPI) and cellular retinaldehyde-binding protein (CRALBP) on the oxidation and reduction of retinoids. Biochemistry **44**, 7035–7047

27 Bradford, M. M. (1976) A rapid and sensitive method for the quantitation of microgram quantities of protein utilizing the principle of protein–dye binding. Anal. Biochem. **72**, 248–254
28 Lowry, O. H., Rosebrough, N. J., Farr, A. L. and Randall, R. J. (1951) Protein measurement with the Folin phenol reagent. J. Biol. Chem. **193**, 265–275
29 Gollapalli, D. R. and Rando, R. R. (2003) All-*trans*-retinyl esters are the substrates for isomerization in the vertebrate visual cycle. Biochemistry **42**, 5809–5818
30 Ross, R. and Kariya, B. (1980) Morphogenesis of vascular smooth muscle in atherosclerosis and cell culture. In Handbook of Physiology, Section 2: The Cardiovascular System (Stephen, G., ed.), pp. 69–91, American Physiological Society, Bethesda
31 Bohren, K. M., Page, J. L., Shankar, R., Henry, S. P. and Gabbay, K. H. (1991) Expression of human aldose and aldehyde reductases. Site-directed mutagenesis of a critical lysine 262. J. Biol. Chem. **266**, 24031–24037
32 Noy, N. and Xu, Z. J. (1990) Interactions of retinol with binding proteins: implications for the mechanism of uptake by cells. Biochemistry **29**, 3878–3883
33 Ong, D. E., MacDonald, P. N. and Gubitosi, A. M. (1988) Esterification of retinol in rat liver. Possible participation by cellular retinol-binding protein and cellular retinol-binding protein II. J. Biol. Chem. **263**, 5789–5796
34 Yost, R. W., Harrison, E. H. and Ross, A. C. (1988) Esterification by rat liver microsomes of retinol bound to cellular retinol-binding protein. J. Biol. Chem. **263**, 18693–18701
35 Li, E., Qian, S. J., Winter, N. S., d'Avignon, A., Levin, M. S. and Gordon, J. I. (1991) Fluorine nuclear magnetic resonance analysis of the ligand binding properties of two homologous rat cellular retinol-binding proteins expressed in Escherichia coli. J. Biol. Chem. **266**, 3622–3629
36 Malpeli, G., Stoppini, M., Zapponi, M. C., Folli, C. and Berni, R. (1995) Interactions with retinol and retinoids of bovine cellular retinol-binding protein. Eur. J. Biochem. **229**, 486–493
37 Wang, J., Chai, X., Eriksson, U. and Napoli, J. L. (1999) Activity of human 11-*cis*-retinol dehydrogenase (Rdh5) with steroids and retinoids and expression of its mRNA in extra-ocular human tissue. Biochem. J. **338**, 23–27
38 Jurukovski, V., Markova, N. G., Karaman-Jurukovska, N., Randolph, R. K., Su, J., Napoli, J. L. and Simon, M. (1999) Cloning and characterization of retinol dehydrogenase transcripts expressed in human epidermal keratinocytes. Mol. Genet. Metab. **67**, 62–73
39 Matt, N., Schmidt, C. K., Dupe, V., Dennefeld, C., Nau, H., Chambon, P., Mark, M. and Ghyselinck, N. B. (2005) Contribution of cellular retinol-binding protein type 1 to retinol metabolism during mouse development. Dev. Dyn. **233**, 167–176
40 Molotkov, A., Ghyselinck, N. B., Chambon, P. and Duester, G. (2004) Opposing actions of cellular retinol-binding protein and alcohol dehydrogenase control the balance between retinol storage and degradation. Biochem. J. **383**, 295–302
41 Harrison, E. H., Blaner, W. S., Goodman, D. S. and Ross, A. C. (1987) Subcellular localization of retinoids, retinoid-binding proteins and acyl-CoA: retinol acyltransferase in rat liver. J. Lipid Res. **28**, 973–998
42 Scott, Jr, W. J., Walter, R., Tzimas, G., Sass, J. O., Nau, H. and Collins, M. D. (1994) Endogenous status of retinoids and their cytosolic binding proteins in limb buds of chick vs mouse embryos. Dev. Biol. **165**, 397–409
43 Molotkov, A., Deltour, L., Foglio, M. H., Cuenca, A. E. and Duester, G. (2002) Distinct retinoid metabolic functions for alcohol dehydrogenase genes *Adh1* and *Adh4* in protection against vitamin A toxicity or deficiency revealed in double null mutant mice. J. Biol. Chem. **277**, 13804–13811
44 Haselbeck, R. J., Ang, H. L. and Duester, G. (1997) Class IV alcohol/retinol dehydrogenase localization in epidermal basal layer: potential site of retinoic acid synthesis during skin development. Dev. Dyn. **208**, 447–453
45 Yamamoto, H., Simon, A., Eriksson, U., Harris, E., Berson, E. L. and Dryja, T. P. (1999) Mutations in the gene encoding 11-*cis* retinol dehydrogenase cause delayed dark adaptation and fundus albipunctatus. Nat. Genet. **22**, 188–191
46 Janecke, A. R., Thompson, D. A., Utermann, G., Becker, C., Hübner, C. A., Schmid, E., McHenry, C. L., Nair, A. R., Rüschendorf, F., Heckenlively, J. et al. (2004) Mutations in RDH12 encoding a photoreceptor cell retinol dehydrogenase cause childhood-onset severe retinal dystrophy. Nat. Genet. **36**, 850–854
47 Tryggvason, K., Romert, A. and Eriksson, U. (2001) Biosynthesis of 9-cis-retinoic acid *in vivo*. The roles of different retinol dehydrogenases and a structure–activity analysis of microsomal retinol dehydrogenases. J. Biol. Chem. **276**, 19253–19258
48 Herr, F. M., Li, E., Weinberg, R. B., Cook, V. R. and Storch, J. (1999) Differential mechanisms of retinoid transfer from cellular retinol binding proteins types I and II to phospholipid membranes. J. Biol. Chem. **274**, 9556–9563
49 Penning, T. M. (2005) AKR1B10: a new diagnostic marker of non-small cell lung carcinoma in smokers. Clin. Cancer Res. **11**, 1687–1690
50 Petrash, J. M. (2004) All in the family: aldose reductase and closely related aldo-keto reductases. Cell. Mol. Life Sci. **61**, 737–749

Received 15 December 2005/11 May 2006; accepted 21 June 2006
Published as BJ Immediate Publication 21 June 2006, doi:10.1042/BJ20051988